

# Mechanism of Void Formation in Cable Covering

G. TITOMANLIO and S. PICCAROLO, *Istituto di Ingegneria Chimica, Palermo, Italy*

## Synopsis

Solidification after extrusion of coaxial cables has been experimentally simulated. Solidification tests were performed with two HDPE grades and under several pressures; the extrusion velocity was varied in a suitable range so as to detect the critical velocity for void formation. A qualitative analysis of the void formation mechanism is carried out, and the predicted trends favorably compare with the critical velocity data.

## INTRODUCTION

Usually coaxial cables are obtained by extruding a polymeric insulating material over a metal center conductor.

As the outer part of the polymer solidifies first, the inner region cannot undergo freely the volume decrease related to solidification. In the absence of a compensating mechanism, the adhesion of the plastic to the metal would be very low and macroscopic voids would form within the polymer,<sup>1,2</sup> thus reducing the dielectric strength and permittivity of the material.<sup>3</sup>

Systematic data on void formation in the cable covering process are not available in the literature. A simple laboratory technique has been used in this work to simulate the cooling after extrusion.

Although the experimental situation differs in some ways from the actual process, the data obtained outline trends which can be a qualitative guide also in the process situation.

The experimental results are compared with the predictions of a physical model for void formation recently developed with reference to the cooling after extrusion of polymeric bars.<sup>4</sup>

## EXPERIMENTAL

The cooling after extrusion in cable covering was simulated by means of the apparatus schematically shown in Figure 1. It was designed and the operating conditions were chosen so as to easy control the "processing conditions" and their reproducibility. The experimental set up was made of three major parts: a cooling bath, a vertical oven located over the bath, and a glass cylinder with a brass rod fastened at its axis and filled with molten polymer. Inside the oven the polymer was molten and compacted under vacuum (in order to avoid gas bubbles in the melt) by a spring driven piston. After the melt was compacted the piston was removed and a gas pressure was applied, and maintained constant until the experiment end. The glass cylinder was then moved downward with constant velocity, through a hole in the bottom of the oven, into the cooling bath thus simulating the extrusion of a cable.

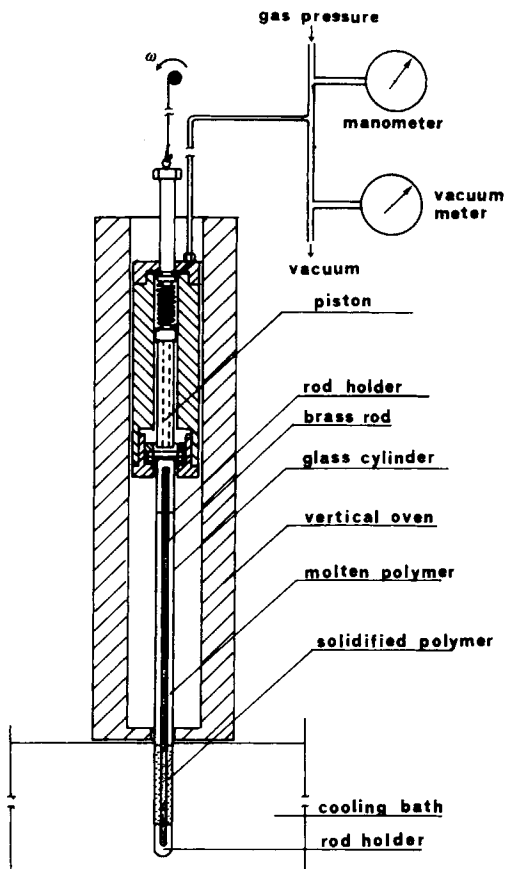


Fig. 1. Schematic drawing of the apparatus.

of a cable.

Two grades of high density polyethylene (HDPE) having zero shear viscosity  $\eta$  at  $140^{\circ}\text{C}$  of  $3 \times 10^5$  and  $4 \times 10^4$  P and the same activation energy were adopted for the tests.

The presence of voids, in the samples obtained after the cooling tests, was detected by X-ray photographs. When present, voids were always located very close to the center brass rod. The minimum void dimension which could be detected with this technique was estimated to be about 0.05 cm.

The oven and the cooling bath temperatures were held at  $200^{\circ}\text{C}$  and  $0^{\circ}\text{C}$ , respectively, for all the tests. The glass cylinder had internal radius  $R$  0.62 cm and wall thickness 0.12 cm; brass rods of radii 0.2 and 0.3 cm were used.

Tests were performed at 1, 3, and 9 ata for both rod diameters. This might appear surprising as the process usually is not performed under pressure, but, as will appear in the following analysis, a pressure increase is essentially equivalent to a viscosity decrease.

## RESULTS

The solid samples obtained after the cooling tests did not adhere to the glass wall, and their diameters were only slightly smaller than the internal

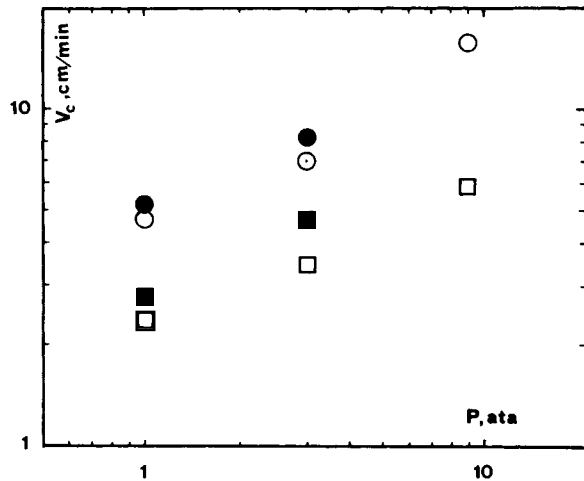


Fig. 2. Critical velocity  $V_c$  vs. operating pressure.  $\eta$  and  $r_b$  are zero shear viscosity and radius of internal rod, respectively.

$r_b$ (cm)	$\eta$ (P)	
	$3 \times 10^5$	$4 \times 10^4$
0.3	■	●
0.2	□	○

diameter of the glass cylinder (both measured at room temperature). As the small difference was compatible with that between the glass and solid polymer thermal expansion coefficients, it was concluded that the polymer remained in contact with the glass wall throughout the cooling process.

For each choice of polymer, pressure  $P$  and brass rod radius  $r_b$ , the "extrusion" velocity  $V$  was varied in a suitable range. At sufficiently low velocities, no voids were found and the adhesion of the polymer on the brass rod was complete; indeed after solidification large forces had to be applied to slide the rod out of the polymer shell. Usually voids formed in the solid polymer by effect of a sufficient increase of the extrusion velocity. A critical velocity  $V_c$ , corresponding to the onset of void formation, as revealed by X-ray photographs, was thus determined.

In a few cases, all taking place when the larger diameter rod was used, a local detachment of the solidified polymer from the center rod was observed on increasing the extrusion velocity. This phenomenon reduces the system density and thus is a competing mechanism to void formation inside the polymer which, consequently, in these cases, either takes place under still larger velocities or completely disappears. The onset of the detachment depends upon the chemical nature and roughness of the solid surface and its study is beyond the purpose of this work.

The critical velocity data are shown in Figure 2 for all the experimental conditions considered, but the tests performed at 9 ata with the larger diameter rod, as in these cases the detachment was *clearly* identified. The results in Figure 2 show that  $V_c$  increases with the operating pressure  $P$  and decreases as the melt viscosity increases. Furthermore, the data in-

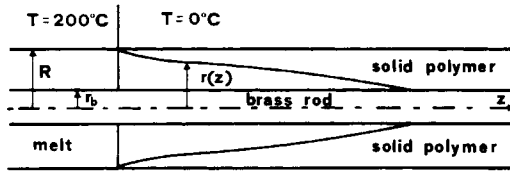


Fig. 3. Scheme of the solidification front.

dicating a pressure dependence slightly smaller for the high viscosity than for the low viscosity polymer; in the latter case  $V_c$  appears to be essentially proportional to  $P^{1/2}$ .

Finally, for a given pressure and polymer, higher critical velocities were systematically obtained when the larger diameter brass rod was used.

### ANALYSIS AND DISCUSSION

A scheme of the sample solidification process is shown in Figure 3. When the sample enters the cooling bath, polymer solidification starts from the outer part and gradually penetrates toward the center. A solidification front, stationary in space, will form in the polymer; its length is expected to increase with the sample advancing velocity.

The density increase due to the material solidification has the effect of decreasing the pressure inside the cavity bounded by the solidification front, and thus a compensating flow arises which is driven by the difference in pressure. If the compensating flow is sufficient to prevent absolute pressure in the cavity dropping to zero, voids will not form. Otherwise, voids tend to form, their growth toward detectable dimensions is favored by the further pressure drop which takes place as the void approaches the tip of the cavity and is hindered by the viscous resistance of the medium.

In the actual cable covering process the extruded polymer is cooled in a more gradual way, by using a cooling trough held at temperatures close to 80°C and located somewhat remote from the die. Furthermore, the polymer is sandwiched between the glass cylinder and the brass rod center conductor in our experiment whereas it is not constrained on the outer radius in the usual extrusion. These differences affect both the cavity length and the pressure at the cavity entrance. The latter coincides with the operating pressure in the real process while it decreases by effect of the pressure drop between the glass wall and the brass rod in our experiment where void formation is thus favored. The former increases by effect of a higher temperature of the cooling bath and can decrease remarkably if the temperature upstream to the cooling bath becomes very close to the crystallization temperature.

The mechanism of void formation is, however, the same both in the experiment and in the actual process. A description of the phenomena involved, with reference to the extrusion of polymer rods, was recently presented.<sup>4</sup> This physical model is here adopted and developed devoting attention to the cable covering process rather than to the experimental situation.

The average velocity  $\langle V \rangle$  of the compensating flow inside the cavity can be easily obtained by a mass balance

$$\langle V \rangle = \beta V \quad (1)$$

where

$$\beta = \frac{\rho_s - \rho_m}{\rho_m} \quad (2)$$

is the fractional volume contraction coefficient upon solidification which, for the polymers adopted here, was  $\beta \simeq 0.25$ .

### Pressure Drop in the Cavity

The pressure drop associated to the compensating flow is here considered assuming Newtonian behavior. If the length of the solidification front along the axial direction  $z$  is sufficiently larger than the cavity thickness (this point will be considered below), the equation for laminar flow through an annulus can be adopted for the pressure gradient:

$$\frac{dp}{dz} = - \frac{8\eta\beta V}{[1 + K^2 + (1 - K^2)/\ln K]r(z)} \quad (3)$$

where  $r(z)$  describes the solidification front and

$$K = \frac{r_b}{r(z)} \quad (4)$$

describes locally the annulus dimensions. Obviously, in order to integrate eq. (3) the function  $r(z)$  has to be specified.

The solidification front profile  $r(z)$  depends on thermal properties of both polymer and central brass rod and on the system geometry  $R$  and  $r_b$ ; furthermore, its length certainly increases with the extrusion velocity. The heat transfer problem for the case of the extrusion of polymer rods<sup>4</sup> was solved numerically, neglecting axial conduction, and the solidification front was found to be closely described by an equation of the type

$$\frac{r(z)}{R} = A \left(1 - \frac{z}{L}\right)^m \quad (5)$$

where  $A$  and  $m$  are constants and  $L$  has the meaning of the cavity length given by

$$L = \frac{VR^2}{\alpha} l \quad (6)$$

$\alpha$  being the solid polymer thermal diffusivity and  $l$  a dimensionless cavity length.  $A$ ,  $m$ , and  $l$  depend upon both Stefan number and a normalized solidification temperature; for the polymers and the temperatures adopted in Ref. 4 (which coincide with those adopted here)  $A$ ,  $m$ , and  $l$  were 0.94, 0.8, and 0.66, respectively.

The problem we are concerned with is different with respect to the extrusion of a rod because of two main reasons which affect the cavity length in opposite directions. The cavity tends to be shorter because it does not involve the whole radius  $R$  but only the polymer annulus. It tends to become larger because the heat to be removed through the polymer shell is larger due to the different volumetric heat capacities of the brass rod and the solid polymer. If the cavity remains of the same order as that of the polymer rod having the same diameter, one has

$$\frac{L}{R} = O\left(\frac{VR}{\alpha}\right) \quad (7)$$

For the data reported in Figure 2

$$11 < \frac{VR}{\alpha} < 80 \quad (8)$$

which corresponds to cavities having length sufficiently larger than the thickness as was previously hypothesized.

In order to obtain a detailed description of the cavity, as required for the integration of eq. (3), the thermal problem should be solved also in this case; unfortunately, axial conduction cannot be neglected in the central brass rod. Thus, solving numerically the problem becomes a very difficult task, which is beyond the purpose of this work. However, taking the cavity length proportional to the extrusion velocity, one has for  $K$

$$K = K(\zeta, b) \quad (9)$$

where

$$b \equiv \frac{r_b}{R} \quad (10)$$

and  $\zeta$  can be written as

$$\zeta = \frac{z\alpha}{VR^2} d \quad (11)$$

where  $d$  replaces  $1/l$  in eq. (6) and can be considered function only of the system geometry, that is, of  $b$ . As mentioned in the previous section, the cavity length, and thus  $d$ , is a function of the operating temperatures.

The pressure drop inside the cavity can now be formally obtained from eq. (3), in particular the axial dimensionless position  $\zeta_0$ , where the pressure drops to zero and a microvoid starts to grow is determined by the equation

$$Z \equiv \frac{P\alpha}{\eta V^2} = \frac{8\eta \beta R^2}{dr_b^2} \int_0^{\zeta_0} \frac{K^2(\zeta, b)}{F(K)} d\zeta \tag{12}$$

where  $P$  is the pressure at the cavity entrance and  $F(K)$  is

$$F(K) = 1 + K^2 + (1 - K^2)/\ln K \tag{13}$$

**Void Growth**

Downstream to the zero pressure position  $\zeta_0$  the void growth is hindered by the viscous resistance of the medium. Neglecting surface tension, the growth is a spherical void having diameter  $D$  in a Newtonian medium of negative pressure  $p(t)$  is described by the equation

$$4\eta \frac{d \ln D}{dt} = -p(t) \tag{14}$$

As voids were detected always very close to the brass rod, the growing void moves with the brass velocity  $V$  and its displacement is  $dz = V dt$ . Thus eq. (14) can be written as

$$\frac{\alpha^2}{V^2 R^2} \frac{d \ln D}{d\zeta} = \frac{2R^2\beta}{d^2r_b^2} \int_{\zeta_0}^{\zeta} \frac{K^2(\zeta, b)}{F(K)} d\zeta \tag{15}$$

Equation (15) has to be integrated from  $D_1$ , the characteristic initial dimension of a nucleating void, to  $D_2$ , the final void dimension. Correspondingly,  $\zeta$  varies from  $\zeta_0$  to  $\zeta_2$ , which is the value where the local transverse dimension of the cavity is of order  $D_2$ . The equation which determines the critical velocity is thus obtained:

$$\frac{1}{Y} \ln \frac{D_2}{D_1} = \frac{2R^2\beta}{d^2r_b^2} \int_{\zeta_0}^{\zeta_2} \int_{\zeta_0}^{\zeta} \frac{K^2(\omega, b)}{F(K)} d\omega d\zeta \tag{16}$$

where

$$Y = \frac{V_c R}{\alpha} \tag{17}$$

$\zeta_0$  is identified by eq. (12) and  $\zeta_2$  is a constant defined by

$$K_2 \equiv \frac{r_b}{r_b + D_2} = K(\zeta_2, b) \tag{18}$$

The group  $Y$  has to be considered a function of  $Z$  and  $\zeta_2$ .  $Z$  can obviously be replaced by any power combination of  $Y$  and  $Z$  itself:

$$X = ZY^2 = \frac{PR^2}{\alpha\eta} \quad (19)$$

has the advantage it does not contain the unknown  $V_c$ . The pressure  $P$  coincides with the operating pressure in the actual process. On a qualitative basis it can be replaced by the operating pressure also in our experiment; this simplification means overestimating the value of  $X$ .

In conclusion, eq. (16) states that at the critical conditions for void formation  $Y$  is a function of  $\zeta_2$ ,  $\zeta_0$ , and  $b$ . As  $\zeta_0$  is a function of  $z$  and  $b$  through eq. (12), accounting for eq. (19), one has

$$Y = Y(X, \zeta_2, b) \quad (20)$$

### Limiting Behaviors and Qualitative Comparison

The function  $K^2/F$  which appears in the integrals on the right-hand side of eqs. (12) and (16) is a dimensionless axial pressure gradient. It certainly grows with  $\zeta$ , as the cavity thickness decreases, but it remains bounded as, at the final position  $\zeta_2$ , the annulus (cavity) has a nonzero thickness.

Once this has been recognized, limiting behaviors can be easily associated with the extreme values of  $\zeta_0$ , i.e., zero and  $\zeta_2$ . For sufficiently small values of  $\zeta_0$  (and  $Z$ ), i.e., when voids nucleate at the entrance of the cavity, the integral on the right-hand side of eq. (16), and thus  $Y$ , become constant as  $Z$  and  $X$  decrease. Contrary to what is shown by the data reported in Figure 2, in this zone the critical velocity is predicted not to be influenced by pressure and viscosity.

All data of Figure 2 are plotted in Figure 4 as  $Y$  vs.  $X$ . In this plot one curve for each value of the brass rod diameter can be identified, although some scatter is shown by the points (closed symbols) relative to the larger rod, which, as mentioned in Experimental, may be due to some undetected detachment between the polymer and the center rod. Vice versa, the points obtained using the smaller rod (open symbols) appear to have a very regular behavior, thus confirming that  $X$  is the group regulating the phenomenon. In particular, consistently with the limiting behavior identified in the limit

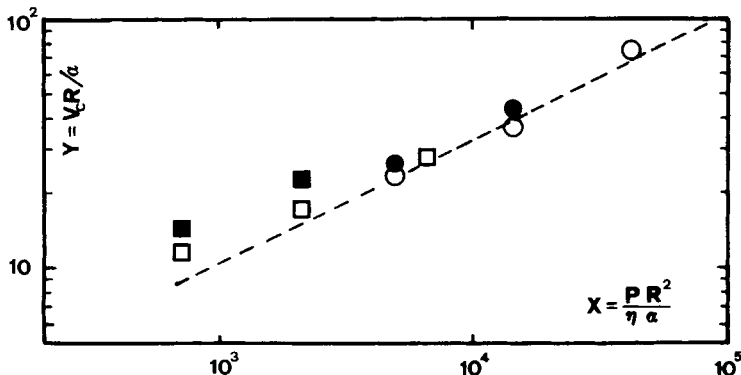


Fig. 4. Normalized critical velocity diagram. Key to symbols as in Figure 2. Dotted line indicates 0.5 slope.



of small  $X$ , the slope of the curve of  $Y$  vs.  $X$  decreases as  $X$  decreases. Furthermore, a straight line of slope 0.5, i.e.,  $Y \propto X^{1/2}$ , becomes a good approximation to the data for large values of  $X$ . This slope corresponds to the other limiting behavior, that for  $\zeta_0$  sufficiently close to  $\zeta_2$ , which means voids starting to nucleate very close to their solidification. In this limit  $Z$  becomes constant and  $Y$  grows indefinitely according to the following limiting form of eq. (16):

$$Y = \frac{bd}{K_2} \left[ \frac{F(K_2)}{\beta \ln(D_2/D_1)} \right]^{1/2} \frac{1}{\zeta_2 - \zeta_0} \quad (21)$$

The relation between  $Y$  and  $X$  is obtained from eq. (19), which indeed shows that in the limit of  $Z$  being constant  $Y$  becomes proportional to  $X^{1/2}$  as shown by the data in Figure 4.

The details of the cavity profile need to be known in order to investigate the effect of  $r_b$  on the critical velocity.

### CONCLUDING REMARKS

Void formation mechanism in cable covering has been qualitatively analyzed. The groups regulating the phenomenon have been identified, and the trends shown by the data of critical extrusion velocity as a function of both operating pressure and melt viscosity have been associated with the limiting behavior of the model equations.

For a more quantitative analysis, knowledge of the solidification front profile is required. To this purpose, the heat transfer problem should be solved, accounting for convection and both radial conduction and latent heat in the polymer and, in the center metal element, of both axial conduction and convection. The values of critical velocity for void formation could thus be calculated by means of eqs. (12) and (16), and the range of validity for the limiting behaviors identified here could be quantitatively defined.

Also non-Newtonian effects, which have been neglected in the analysis, can play some relevant role.

Data of critical velocity for void formation taken in a model experiment are considered for qualitative comparison. The predicted trends are reproduced by the experiment.

This work has been supported by MPI.

### References

1. J. H. Daane, "Factors affecting the grip of dielectric core within submarine coaxial cables," *Proceedings of the XXIV International Wire and Cable Symposium*, Cherry Hill, N. J., November 1975, p. 75.
2. R. M. Fairfield and F. J. Cox, in *Polythene*, A. Renfrew and P. Morgan, Eds., Wiley-Interscience, New York, 1960, Chap. 19.
3. W. Heckman and J. Schiag, *Kunststoffe* **72**, 96 (1982).
4. G. Titomanlio, S. Piccarolo, and G. Marrucci, *Polym. Eng. Sci.*, to appear.

Received December 2, 1983

Accepted November 13, 1984